Scientific Research Publishing

Open Journal of Applied Sciences, 2024, 14, 2482-2505
https://www.scirp.org/journal/ojapps
ISSN Online: 2165-3925
ISSN Print: 2165-3917

Exploration on the Optimization Strategy for the Layup of Composite Material Pressure Vessels Based on Advanced Algorithms

Qingshan Zeng, Zuxin Chen

School of Aircraft Engineering, Nanchang Hangkong University, Nanchang, China
Email: 2937101018@qq.com

How to cite this paper: Zeng, Q.S. and Chen, Z.X. (2024) Exploration on the Optimization Strategy for the Layup of Composite Material Pressure Vessels Based on Advanced Algorithms. *Open Journal of Applied Sciences*, **14**, 2482-2505.
https://doi.org/10.4236/ojapps.2024.149164

Received: August 10, 2024
Accepted: September 10, 2024
Published: September 13, 2024

Abstract

This study aims to explore the influence of the laying angle on the pressure shell structure made of composite materials under the condition of a fixed shape. By using a composite material composed of a mixture of T800 carbon fiber and AG80 epoxy resin to design pressure vessels, this material combination can significantly improve the interlaminar shear strength and heat resistance. The article elaborates on the basic concepts and failure criteria of composite materials, such as the maximum stress criterion, the maximum strain criterion, the Tsai-Hill criterion, etc. With the help of the APDL parametric modeling language, the arc-shaped, parabolic, elliptical, and fitting curve-shaped pressure vessel models are accurately constructed, and the material property settings and mesh division are completed. Subsequently, APDL is used for static analysis, and the genetic algorithm toolbox built into Matlab is combined to carry out optimization calculations to determine the optimal laying angle. The research results show that the equivalent stress corresponding to the optimal laying angle of the arc-shaped pressure vessel is 5.3685e+08 Pa, the elliptical one is 5.1969e+08 Pa, the parabolic one is 5.8692e+08 Pa, and the fitting curve-shaped one is 5.36862e+08 Pa. Among them, the stress distribution of the fitting curve-shaped pressure vessel is relatively more uniform, with a deformation of 0.568E−03 m, a minimum equivalent stress value of 0.261E+09 Pa, a maximum equivalent stress value of 0.537E+09 Pa, and a ratio of 0.48, which conforms to the equivalent stress criterion. In addition, the fitting curve of this model can adapt to various models and has higher practical value. However, the stress distribution of the elliptical and parabolic pressure vessels is uneven, and their applicability is poor. In the future, further exploration can be conducted on the application of the fitting curve model in composite materials to optimize the design of pressure vessels. This study provides important theoretical support and practical guidance for the design of

composite material pressure vessels.

Keywords

Composite Material Pressure Vessel, Matlab, APDL Parametric Modeling, Static Analysis, Optimal Laying Angle

1. Introduction

This paper conducts an in-depth exploration into the relevant issues concerning the design of pressure vessels using the composite material formed by blending T800 carbon fiber with AG80 epoxy resin. The research results clearly reveal that the incorporation of a small amount of AG80 epoxy resin into T800 carbon fiber can significantly enhance the interlaminar shear strength and heat resistance. This improvement has a significant advantage compared to the use of a single resin, fully demonstrating the synergistic effect between the materials. Based on the characteristics of the aforementioned materials, this paper will carry out an in-depth and systematic study based on this foundation.

In addition, APDL parametric modeling has the ability to accurately construct pressure vessel models of various shapes, determine material properties, and reasonably divide the mesh, providing an accurate model basis for subsequent analysis. As a random global search optimization method, the genetic algorithm, when combined with APDL, can call the APDL program through MATLAB to retrieve and calculate variables, so as to determine the optimal layup angle and corresponding equivalent stress value for pressure vessels of different shapes under the constraints of relevant conditions. Furthermore, through comparative analysis, it is found that the fitting curve-shaped pressure vessel model shows higher practical value when considering the layup angle in composite materials because its fitting curve can adapt to various models, including parabolas, arcs, ellipses, etc., and can make the stress distribution of the pressure vessel relatively uniform, which conforms to the equivalent stress criterion.

The central aim of this research is to thoroughly investigate the mechanical performance of composite material pressure vessels with different shapes at various layup angles, accurately ascertain the optimum layup angle, in order to effectively boost the safety, reliability, and service life of pressure vessels. At the same time, it intends to offer solid theoretical and practical guidance for the design and fabrication of composite material pressure vessels.

Yohannes Regassa [1] used finite element modeling to evaluate the composite wound pressure vessel with a 4-mm-thick aluminum-core cylinder. By designing many models and deeply analyzing the variable relationships, it was concluded that the stacking sequence of the laminate in the [55˚, −55˚] PP winding mode has the best COPV design profile, and its burst pressure bearing capacity reaches 24 MPa. Moreover, the stress-strain distribution and law along the COPV geometry

were obtained, which greatly assists in the design and application of the composite wound pressure vessel. Young H. Park [2] pointed out in his own research that anisotropic composite cylinders and pressure vessels are widely used in many fields due to their performance advantages. Given that the performance of composite materials depends on the strength in the fiber direction, it is necessary to optimize the design of the composite laminate, and at the same time develop a mathematical three-dimensional elastic solution to calculate the stress, introduce a rotation variable to handle the torsional load, use the three-dimensional Tsai-Wu criterion to predict failure, and adopt a global optimization algorithm to find the best fiber orientation combination. Muhammad Imran [3] carried out design optimization work for the composite underwater pressure-resistant hull under 3 MPa hydrostatic pressure in his research. He used three kinds of unidirectional composite materials, used the genetic algorithm in ANSYS Workbench to optimize the number of layers and orientation angles of various layers, set the minimization of the buoyancy coefficient as the goal, and was subject to various conditions. At the same time, he also used other software for research and carried out sensitivity analysis. Mohammad Hadi Hajmohammad [4] developed a new method to obtain the best fiber orientation in the design of fiber-reinforced polymer pressure vessels. This method covers analysis and optimization, regards many factors as constraints, uses multiple criteria to analyze failure situations, uses genetic algorithms to achieve the best mode, analyzes the influence of functions, and verifies it through experiments. The results show that the critical buckling load increases by 40% and the weight decreases by 15%.

E Fathallah [5] indicated in his research that the design of the laminated composite submarine pressure hull depends on the number of layers and the fiber orientation angle. This study conducted a detailed overview and comprehensive exploration of the multi-objective optimization of the submarine pressure hull under hydrostatic pressure, constructed three models, used low-density PVC foam as the core material, and optimized it in ANSYS, following relevant criteria. The research results show that the carbon/epoxy resin (USN-150) submarine has more superior performance, and the performance with the core layer is better. Finally, an optimized model is given to provide valuable references for future designs. J. Sakai [6] pointed out that anisotropic composite cylinders and pressure vessels are widely used in many fields due to their performance advantages, and pipelines are examples of their applications. Given that the performance of composite materials depends on the strength in the fiber direction, it is necessary to optimize the design of the composite laminate to reduce damage. This study developed a mathematical three-dimensional elastic solution that can accurately calculate the stress, introduced a rotation variable to handle the torsional load, used the three-dimensional Tsai-Wu criterion to predict failure, and used a global optimization algorithm to find the best fiber orientation combination. Chi Wu [7] developed a discrete topology optimization program for the synchronous design of the ply orientation and thickness of the carbon fiber reinforced plastic laminated structure in his own research. By suppressing the intermediate voids through specific

methods, developing algorithms, conducting comparisons and applications, and making prototype tests, the results show that this synchronous optimization method is effective.

A. Vafaeesefat [8] proposed a multi-layer optimization strategy for composite pressure vessels with non-metallic linings. There are numerous design variables, and the objective function is introduced. The algorithm uses genetic algorithms and finite element analysis, and the program is implemented in geodesic and ellipsoidal heads. The results show that the geodesic head with a 9-degree spiral winding has better performance under specific conditions. Kelvin Masakazu Kuroki Iwasaki [9] pointed out that cylindrical pressure vessels have disadvantages and proposed a new method to optimize the design of composite pressure vessels in his own research. Using a thin-walled elliptical head, adopting the gradient method and related software, it meets the design constraints and safety factors, and the number of layers in the optimal sequence is reduced. This method is helpful for the development of the design. Helio Matos [10] pointed out that deep-sea structures below the instability threshold will collapse under hydrostatic pressure. In his own research, he discussed the optimal critical collapse pressure of the composite cylinder under hydrostatic load, combined with previous results to study different configurations and material properties. The results show that the optimal ply configuration is unique but has a general trend, and the proposed analysis method can determine the optimal ply angle of the thin composite cylindrical structure. In this review written by authors including Rony Mia [11], the emphasis is placed on the fabrication of composite materials derived from certain natural source macromolecules. Various types of macromolecules are present in different fibers, and the article primarily describes wood-, silk-, and wool-based macromolecules, concluding that natural macromolecule composite materials possess significant potential for application in diverse fields. This study conducted by Oludele Adeyefa and Oluleke Oluwole [12] aims to ascertain the thickness requirements of large spherical liquefied natural gas (LNG) pressure vessels fabricated on-site through the finite element method. They employed shallow triangular elements and the area coordinate system for modeling and analysis, and the results indicated that the membrane thickness of the LNG container decreased gradually from the bottom upward, while the thickness of the compressed gas container remained constant. Furthermore, the obtained results showed no significant difference from the values of the ASME standard, thus verifying the validity of the model.

Yohannes Regassa evaluated the composite wound pressure vessel with a specific aluminum-core cylinder and obtained the optimal winding mode. Young H. Park pointed out that anisotropic composite cylinders and pressure vessels are widely used and the design of laminate plates needs to be optimized. Muhammad Imran carried out design optimization for underwater pressure-resistant hulls. Mohammad Hadi Hajmohammad developed a new method to optimize fiber orientation. E Fathallah explored the multi-objective optimization of laminated composite submarine pressure-resistant hulls. J. Sakai emphasized optimizing the

design to reduce damage. Researchers have studied composite material pressure vessels from multiple aspects and all presented their own research results. However, not many researchers have focused on aspects such as angles, especially the influence of different laying angles on the stress situation. In this study, the changes of pressure vessels caused by the changes of research angles will be discussed.

2. The Basic Concept of Composite Materials

Composite materials usually consist of two components: the matrix and the reinforcing material. The matrix material can be various resins, metals or non-metallic materials. In composite materials, the reinforcing material is usually made of various fibers or other types of materials. The reinforcing material plays a vital role in composite materials as it provides the stiffness and strength of the composites. The matrix material plays an important role in composite materials, including supporting and fixing the fiber materials, transferring loads between the fibers, and protecting the fibers. Therefore, choosing the appropriate matrix material can significantly improve the specific properties of composite materials. For example, if it is necessary to reduce the density, resin can be selected as the matrix material; if it is necessary to have high-temperature resistance, ceramics can be selected as the matrix material; to obtain higher toughness and shear strength, metals are generally considered as the matrix material.

The performance of composite materials depends not only on the individual performance of the constituent materials, but also on the interface performance between the matrix material and the reinforcing material. Good adhesion performance between the two can form an ideal interface, which is crucial for improving the stiffness and strength of composite materials. The performance of different reinforcing fiber and matrix combinations is listed in Table 1. Among them, PEEK represents polyether ether ketone resin, which is a high-toughness thermoplastic resin.

3. Failure Criterion of Composite Materials

3.1. The Maximum Stress Criterion

Based on the in-plane biaxial stress state shown in Figure 1, through coordinate transformation, the stresses $\sigma_L(\sigma_1)$, $\sigma_T(\sigma_2)$ and $\tau_{LT}(\tau_{12})$ in the direction of the principal axes of the material are obtained. The maximum stress criterion holds that the force components in the direction of the principal axes of the material must be less than their respective strength indices, namely:

$$\begin{cases} \sigma_1 < X_t\left(\text{Tensile}\right) \\ \sigma_2 < Y_t\left(\text{Tensile}\right) \\ \left|\sigma_1\right| < X_c\left(\text{Compress}\right) \\ \left|\sigma_2\right| < Y_c\left(\text{Compress}\right) \\ \left|\tau_{12}\right| < S\left(\text{Shear}\right) \end{cases} \tag{1}$$

If one of the above relations does not hold, the material will fail.

Table 1. Combinations of reinforcing fibers and matrices.

Matrix		Reinforcing fiber					
		Glass	Aramid	Carbon	Boron	Silicon carbide	Alumina
Thermosetting resin	Unsaturated polyester resin	⊙	△	△	△	×	×
	Epoxy resin	○	⊙	⊙	⊙	△	○
	Polyimide resin	△	△	○	△	△	○
Thermoplastic resin	PEEK	△	○	○	×	×	△
	General-purpose resin	○	△	△	×	×	×
Metal	Aluminum	×	×	○	○	○	○
	Titanium	×	×	△	○	⊙	○
	Magnesium	×	×	⊙	△	△	△

Note: In the table, ⊙ indicates good, ○ indicates relatively good, △ indicates average, and × indicates poor.

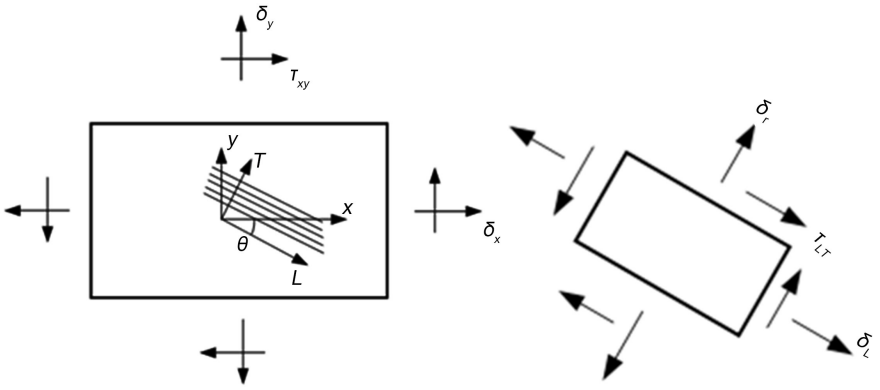

Figure 1. In-plane stressed element.

3.2. The Maximum Strain Criterion

The maximum strain criterion is similar to the maximum stress criterion, except that the components of each stress are replaced by the components of strain, and the corresponding strength indices are replaced by the ultimate strain values, namely:

$$\begin{cases} \varepsilon_1 < \varepsilon_{1t}\,(\text{Tensile}) \\ \varepsilon_2 < \varepsilon_{2t}\,(\text{Tensile}) \\ |\varepsilon_1| < \varepsilon_{1c}\,(\text{Compress}) \\ |\varepsilon_2| < \varepsilon_{2c}\,(\text{Compress}) \\ |\gamma_{12}| < \gamma_{12}^{u}\,(\text{Shear}) \end{cases} \tag{2}$$

As long as one of the same in Formula (2) does not hold, the material will fail.

3.3. Tsai-Hill Criterion

This criterion considers the interaction between the various stress components in the material. The condition for the material not to fail is:

$$F.I.=\left(\frac{\sigma_1}{X}\right)^2+\left(\frac{\sigma_2}{Y}\right)^2+\left(\frac{\tau_{12}}{S}\right)^2-\frac{\sigma_1}{X}\frac{\sigma_2}{X}<1 \tag{3}$$

Unlike the maximum stress criterion, in the Tsai-Hill criterion, the combined influence of each stress component is taken into account, and a failure index *F.I.* is uniformly defined, which is on the left side of Formula (3). When applying this criterion, it can only determine whether failure occurs but not the type of failure. Due to the consideration of the interaction of stress components, situations that are determined not to fail based on the maximum stress criterion might also satisfy the Tsai-Hill failure condition. It should also be noted that this criterion is in principle only applicable to the cases of $X_c = X_t$ and $Y_t = Y_c$.

3.4. Hoffman Criterion

According to this criterion, the condition for the material not to fail is:

$$F.I.=F_1\sigma_1+F_2\sigma_2+F_{11}\sigma_1^2+F_{22}\sigma_2^2+F_{66}\tau_{12}^2+2F_{12}\sigma_1\sigma_2<1 \tag{4}$$

Among them, each strength parameter is determined by the strength index according to the following formulas:

$$F_1=\frac{1}{X_t}-\frac{1}{X_c},\quad F_2=\frac{1}{Y_t}-\frac{1}{Y_c},\quad F_{11}=\frac{1}{X_tX_c} \tag{5}$$

$$F_{22}=\frac{1}{Y_tY_c},\quad F_{66}=\frac{1}{S^2},\quad F_{12}=\frac{1}{2X_tX_c} \tag{6}$$

Similar to the Tsai-Hill criterion, this criterion also considers the interaction between stress components. However, different from the Tsai-Hill criterion, this criterion fundamentally considers the difference between tensile strength and compressive strength.

3.5. Tsai-Wu Stress Criterion

Formally, the Tsai-Wu stress criterion is exactly the same as the Hoffman criterion, that is, the condition for the material not to fail is:

$$F.I.=F_1\sigma_1+F_2\sigma_2+F_{11}\sigma_1^2+F_{22}\sigma_2^2+F_{66}\tau_{12}^2+2F_{12}\sigma_1\sigma_2<1 \tag{7}$$

Among the six strength parameters, the first five parameters are the same as the definitions in Formula (4), except that the definition of F_{12} has changed:

$$F_{12}=\frac{F_{12}^*}{\sqrt{X_tX_cY_tY_c}} \tag{8}$$

The value of coefficient F_{12}^* is between −1 - 1 and is generally taken as $-\frac{1}{2}$.

3.6. The First Floor Failure Strength

For the structure of a common laminated plate, the basis for defining the failure

strength of the first layer is the stress of each layer. Then, it is judged and calculated through the strength criterion. Under normal circumstances, the analysis steps of the failure strength of the first layer in the group are as follows:

1) According to the layup structure of the laminated plate, calculate the stiffness A_{ij}, B_{ij} and D_{ij}.

$$\begin{cases} A_{ij} = \sum_k t_k \left(\overline{Q}_{ij}\right)_k \\ B_{ij} = \sum_k t_k \overline{z}_k \left(\overline{Q}_{ij}\right)_k \\ D_{ij} = \sum_k \left[t_k \left(\overline{z}_k + \frac{t_k^3}{12} \right)^2 \right] \left(\overline{Q}_{ij}\right)_k \end{cases} \tag{9}$$

2) Calculate the flexibility of the laminated plate, and the inversion form of the constitutive relationship can be obtained, that is:

$$\begin{bmatrix} \boldsymbol{N} \\ \boldsymbol{M} \end{bmatrix} = \begin{bmatrix} \boldsymbol{A} & \boldsymbol{B} \\ \boldsymbol{C} & \boldsymbol{D} \end{bmatrix} \begin{bmatrix} \boldsymbol{\varepsilon}^0 \\ \boldsymbol{K} \end{bmatrix} \tag{10}$$

$$\begin{bmatrix} \boldsymbol{\varepsilon}^0 \\ \boldsymbol{K} \end{bmatrix} = \begin{bmatrix} \boldsymbol{A}' & \boldsymbol{B}' \\ \boldsymbol{C}' & \boldsymbol{D}' \end{bmatrix} \begin{bmatrix} \boldsymbol{N} \\ \boldsymbol{M} \end{bmatrix} \tag{11}$$

$$A^* = A^{-1} \tag{12}$$

$$B^* = -A^{-1}B \tag{13}$$

$$C^* = BA^{-1} = -B^{*\mathrm{T}} \tag{14}$$

$$D^* = D - BA^{-1}B \tag{15}$$

$$A' = A^* + B^* D^{*-1} B^{*\mathrm{T}} \tag{16}$$

$$B' = B^* D^{*-1}, C' = B'^{\mathrm{T}}, D' = D^{*-1} \tag{17}$$

In the formula:

$\boldsymbol{N} = \begin{bmatrix} N_x & N_y & N_{xy} \end{bmatrix}^{\mathrm{T}}$ is the internal force per unit width;

$\boldsymbol{M} = \begin{bmatrix} M_x & M_y & M_{xy} \end{bmatrix}^{\mathrm{T}}$ is the bending moment (torque) per unit width;

$\boldsymbol{\varepsilon}^0 = \begin{bmatrix} \varepsilon_x & \varepsilon_y & \gamma_{xy} \end{bmatrix}^{\mathrm{T}}$ is the mid-plane strain of the laminated plate;

$\boldsymbol{K} = \begin{bmatrix} K_x & K_y & K_{xy} \end{bmatrix}^{\mathrm{T}}$ is the mid-plane curvature (bending rate).

If the laying sequence of the laminated plate is symmetrical, then Formulas (10) and (11) can be written as (18) and (19) respectively:

$$\begin{cases} \boldsymbol{N} = A\boldsymbol{\varepsilon}^0 \\ \boldsymbol{M} = \boldsymbol{D}\boldsymbol{K} \end{cases} \tag{18}$$

$$\begin{cases} \boldsymbol{\varepsilon}^0 = \boldsymbol{A}^{-1}\boldsymbol{N} = \boldsymbol{a}\boldsymbol{N} \\ \boldsymbol{K} = \boldsymbol{D}^{-1}\boldsymbol{M} = \boldsymbol{d}\boldsymbol{M} \end{cases} \tag{19}$$

Next, if there is no special explanation, the situation of symmetrical laminated plates is considered.

3) Through Formula (11) or Formula (19), after obtaining ε^0 and K, the strain at any point (any single layer) within the laminated plate can be calculated, that is, the following formula:

$$\begin{bmatrix} \varepsilon_x \\ \varepsilon_y \\ \gamma_{xy} \end{bmatrix} = \begin{bmatrix} \varepsilon_x^0 \\ \varepsilon_y^0 \\ \gamma_{xy}^0 \end{bmatrix} + z \begin{bmatrix} K_x \\ K_x \\ K_{xy} \end{bmatrix} \tag{20}$$

$$\begin{bmatrix} \varepsilon_1 \\ \varepsilon_1 \\ \gamma_{12} \end{bmatrix} = \begin{bmatrix} m^2 & n^2 & mn \\ n^2 & m^2 & -mn \\ -2mn & 2mn & m^2 - n^2 \end{bmatrix} \begin{bmatrix} \varepsilon_x \\ \varepsilon_y \\ \gamma_{xy} \end{bmatrix} \tag{21}$$

4) Calculate the stress of any single layer within the laminated plate:

$$\begin{bmatrix} \sigma_1 \\ \sigma_2 \\ \gamma_{12} \end{bmatrix} = \begin{bmatrix} Q_{11} & Q_{12} & 0 \\ Q_{12} & Q_{22} & 0 \\ 0 & 0 & Q_{66} \end{bmatrix} \begin{bmatrix} \varepsilon_1 \\ \varepsilon_2 \\ \gamma_{12} \end{bmatrix} \tag{22}$$

5) Using the stress components in the single-layer principal axis direction obtained from Formula (22) and substituting them into the corresponding strength criterion to calculate the corresponding failure index (F.I.), the failure strength of the first layer is obtained.

3.7. Optimal Design of Materials and Structures

When conducting optimal design under relevant constraints, by changing the design variables such as the geometric shape or size of the material and structure, to achieve the maximum or minimum value of the objective function. For example, taking the minimum mass as the goal of the optimal design, the lowest cost optimal design, etc. It can be expressed by Formulas (23) and (24):

$$\min F\left(x_1, x_2, \cdots, x_n\right) \tag{23}$$

$$\text{s.t. } g_k\left(x_1, x_2, \cdots, x_n\right) \geq 0 \quad \left(k = 1, 2, \cdots, m\right) \tag{24}$$

The optimal design has three important factors, namely design variable x_i, objective function $F\left(x_1, x_2, \cdots, x_n\right)$ and constraint condition (24). When doing the relevant design, the variable setting among them is a controllable quantity that the designer can change according to the needs in his own design. When designing composite materials, the design itself has considerable flexibility, which is closely related to the stiffness or strength of the composite materials and their various components (such as fibers, aggregate types) and composition structures (lamellar structures). Combining different materials or making various changes to their structures can also freely change the overall performance of the laminated plates very well.

When conducting the optimal design of composite materials, its design variables can be divided from the following aspects:

1) Mechanics or physical properties of materials

2) The geometric structure of the layup

3) The shape of the laminated plate or the size of the cross-section, etc.

Compared with the first type of design variable, different reinforcing materials can be considered to be used, such as carbon fiber, glass fiber and aramid fiber, as well as different matrix materials, such as various resins. Besides, different forms of reinforcing materials can also be chosen, such as unidirectional reinforcement, braided reinforcement, short fiber reinforcement, etc., and the volume fraction of the reinforcing materials can be considered. As for the second design variable, the laying angle and the laying sequence can be considered.

The objective function can be divided into the following types according to the requirements of specific designs:

1) Minimize the mass of the structure

2) Maximize the strength or stiffness of the structure

3) Maximize the reliability of the structure

Constraints can be divided into two categories: One type is design variables, such as the volume fraction of reinforcing materials, the angle of fiber laying and the geometric size of single-layer plates; the other type is the optional range; another type is functional constraints, such as maximum deformation, buckling strength, reliability and other performance indicators that can be satisfied.

4. Establishment of Composite Material Model

4.1. Establishment of the Model

By using the APDL parametric modeling language, this section creates the relevant model and uses the genetic algorithm to optimize the layup angle of the pressure vessel for calculation.

The parametric modeling of the circular arc pressure vessel model is carried out by using Formulas $x^2 + y^2 + Dx + Ey + F = 0$, $\left(-\frac{D}{2}, -\frac{E}{2}\right)$, and $r = \frac{\sqrt{D^2 + E^2 - 4F}}{2}$, as shown in Figure 2:

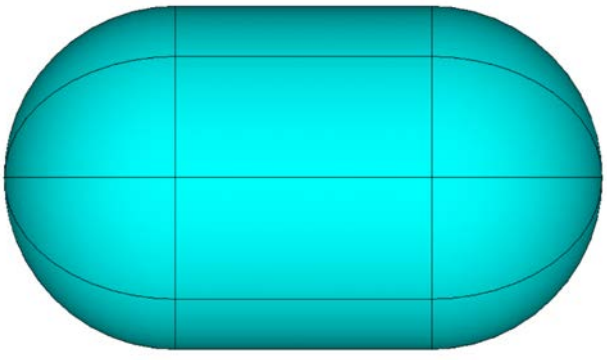

Figure 2. Arc-shaped pressure vessel model.

The parabolic pressure vessel model is parametrically modeled using formulas $y^2 = 2px$ and $y^2 = -2px$, as shown in Figure 3:

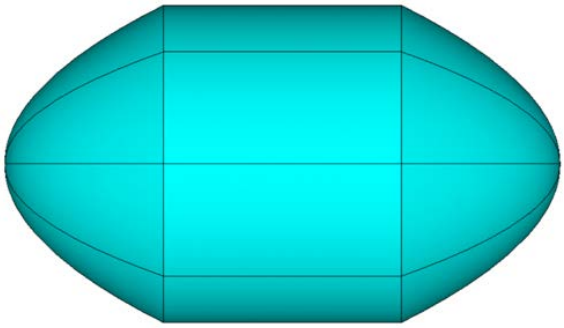

Figure 3. Parabolic pressure vessel model.

Parametric modeling of the elliptical pressure vessel model is carried out using Formulas $\frac{x^2}{a^2}+\frac{y^2}{b^2}=1(a>b>0)$ and $\frac{y^2}{a^2}+\frac{x^2}{b^2}=1(a>b>0)$, as shown in Figure 4:

Figure 4. Elliptical pressure vessel model.

Parametric modeling is conducted on the fitting curve-shaped pressure vessel, and the resulting model diagram is shown in Figure 5:

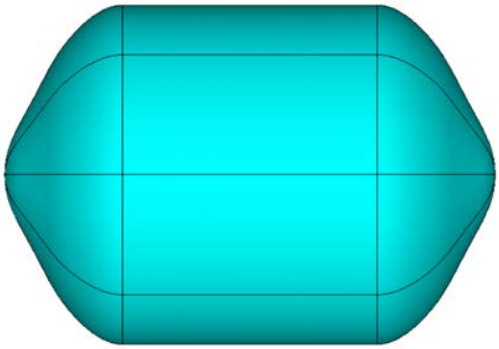

Figure 5. Fitting Curve-shaped pressure vessel model.

4.2. Determination of Material Properties

In this section, the pressure vessel model was constructed. When using APDL in ANSYS, the element type used was first defined as SHELL181. The SHELL181 element is the most suitable one in APDL to describe thin-walled pressure vessels. The materials used in several models are all composite materials composed of a mixture of T800 carbon fibers and AG80 epoxy resin. The Poisson's ratio is set to

0.3, the elastic modulus is set to 150 GPa, and the density is set to 1800 kg/m^3.

The setting method is shown in the code below:

```
MPDATA, EX, SHELL _ MAT _ NUM, 1.5e11
MPDATA, PRXY, SHELL _ MAT _ NUM, 0.3
MPDATA, DENS, SHELL _ MAT _ NUM, 1800
```

4.3. Mesh Division

Mesh division is of crucial importance in finite element analysis because it requires careful consideration of the actual structure, boundary conditions, and problem-solving. The division of the mesh directly affects the accuracy and duration of the calculation. An overly complex division can lead to an excessively long calculation time, while an overly simplistic division can result in inaccurate results. Therefore, it is necessary to precisely divide the mesh of the structural model to obtain accurate results and avoid excessive calculation time.

In the APDL part of ANSYS, it can be achieved by using the element shape command MSHAPE, KEY, Dimension. This command can be used to determine the shape of the mesh. In this section, a 2D tetrahedral element was selected as the mesh of the model. This element was divided into a free mesh and covered the entire model area.

1) The effect picture of the meshing of the circular arc pressure vessel model is shown in Figure 6:

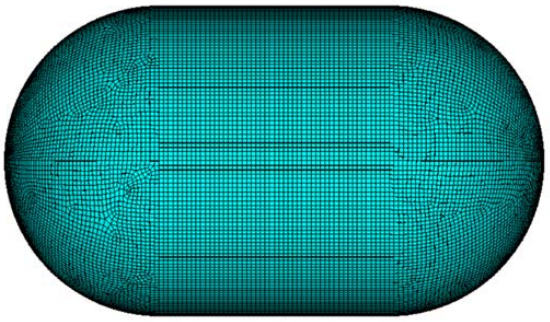

Figure 6. Meshing of the circular arc pressure vessel model.

2) The meshing of the elliptical pressure vessel model is shown in Figure 7: 0.

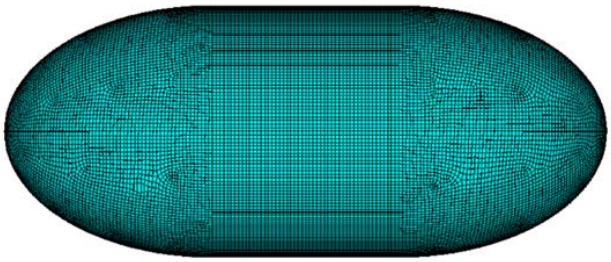

Figure 7. Meshing of the elliptical pressure vessel model.

3) The meshing of the parabolic pressure vessel model is shown in Figure 8:

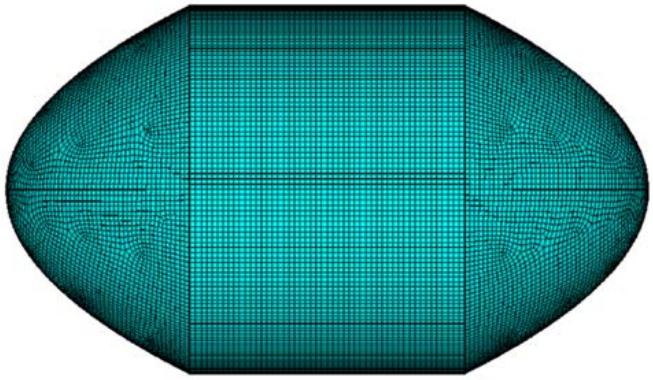

Figure 8. Meshing of the parabolic pressure vessel model.

4) The meshing of the fitting curve-shaped pressure vessel model is shown in Figure 9:

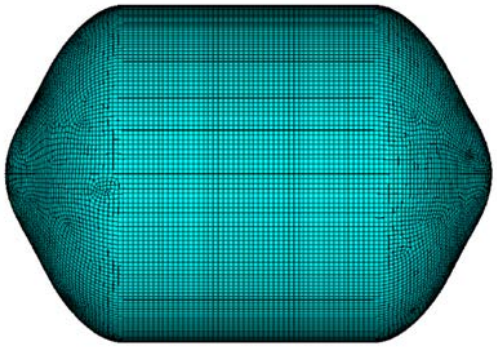

Figure 9. Meshing of the fitting Curve-shaped pressure vessel model.

4.4. The Setting of Ply Parameters

Since the research object is the structure of the composite material pressure vessel, the SHELL181 element type has been introduced in the previous section. The main research goal of this chapter is to optimize the laying angle of the composite material pressure vessel.

In the help documentation of ANSYS, it has been pointed out in the explanation of the SHELL181 element that SECTYPE, SHELL and SECDATA, THICKNESS are used to define the relevant data settings of the ply. Among them:

$$\text{SECTYPE}, \text{SECID}, \text{TYPE}, \text{SUBTYPE}, \text{NAME}, \text{REFINEKEY}$$

This subsection only needs to use the first two blanks. The section number is set to 1, and the selected element type in the model is SHELL. Therefore, the defined and completed command is as follows:

SECTYPE,1,SHELL

SECDATA, VAL1, VAL2, VAL3, VAL4, VAL5, VAL6,
VAL7, VAL8, VAL9, VAL10, VAL11, VAL12

This command was originally used to describe the geometry of the cross-section, and here it is used to define the thickness and angle of a single ply.

Set the total thickness as DQ = 0.008 m. For the four models, a total of eight layers are set. The thickness of each layer is DQ/8. There are a total of eight layers, and the angle of each layer is set as $x_1, x_2, x_3, x_4, x_5, x_6, x_7, x_8$. The constraint condition of the angle is as shown in the following formula (25):

$$0^\circ \le x_i \le 180^\circ \quad (i = 1, 2, \cdots, 8) \tag{25}$$

After the constraint conditions are determined and the parameter values are set, the entire complete command is as follows:

SECT,1,SHELL,,
SECDATA,DQ/8,1, x_1,3
SECDATA,DQ/8,1, x_2,3
SECDATA,DQ/8,1, x_3,3
SECDATA,DQ/8,1, x_4,3
SECDATA,DQ/8,1, x_5,3
SECDATA,DQ/8,1, x_6,3
SECDATA,DQ/8,1, x_7,3
SECDATA,DQ/8,1, x_8,3
SECOFFECT,MID
SECCONTROL,,,,,,,

4.5. The Combined Use of Genetic Algorithm and APDL

The Genetic Algorithm (GA for short) originated from the biological reproduction system, and then began to conduct simulation research using computers. It is a random global search optimization method.

In this section, the APDL program and the genetic algorithm in MATLAB will be combined, and the unique characteristics of the genetic algorithm will be utilized to optimize and find the best solution.

Use MATLAB to call the APDL program to find the answer. The calling code for the following part:

$$\text{gz\_index} = \text{a} : \text{b} \tag{26}$$

Through (26), the variables in the APDL program can be retrieved, where: A and B refer to the positions of the variables in APDL. When dealing with a single variable, only one position needs to be determined; while when dealing with multiple variables, after appropriate processing, these variables can be better called for calculation.

$$\text{fid} = \text{fopen}(\text{'}, \text{'r'}) \tag{27}$$

The name of the APDL program that needs to be called is filled in the middle

of the single quotes.

```
while ~feof(fid)
    tline = fget1(fid)
    i = i + 1
switch i
case gz_index()
tline = [',num2str()]
```
(28)

The first line in (28) represents reading the contents of the text document line by line until the end of reading. The second line of code represents storing the current line as tline. The third line of code represents recording the current stored line number. The fourth line refers to the function of the sixth line of code is to record the next line number and replace the content in the square brackets.

4.6. Analysis Based on the Optimization Results of MATLAB

The setting of relevant data of the genetic algorithm is crucial to the calculation results, and it directly affects the accuracy and speed of optimization calculation using the genetic algorithm. The following are the settings of some data of the genetic algorithm tool.

Since the angle of the ply is optimized, the upper and lower limits of the variables are set as in the following code (29):

$$\begin{aligned} LB &= [0,0,0,0,0,0,0,0] \\ UB &= [180,180,180,180,180,180,180,180] \end{aligned} \tag{29}$$

The settings of the relevant data of the genetic algorithm are as follows: The population size is set at 20, and the total number of iterations is 10,000. The value of the change in the best fitness is set to 1E-06. Other values of the genetic algorithm are set to the default values.

1) Under the constraints of relevant conditions, the circular arc pressure vessel model obtained the optimal laying angle and the corresponding equivalent stress value, as shown in Table 2:

Table 2. Optimal laying angle and equivalent stress magnitude.

x_1	x_2	x_3	x_4	x_5	x_6	x_7	x_8	Equivalent stress (Pa)
127˚	136˚	147˚	136˚	47˚	156˚	72˚	73˚	5.3685e+08

After the optimization calculation of the genetic algorithm, the results as shown in the above chart are presented. Figure 10 shows the schematic diagram of the laying angle of each layer. In APDL, by using the SECPLOT command, the set number of ply layers and laying angles can be retrieved. As shown in Figure 10, the laying angle of the first layer from left to right is: 127˚, the laying angle of the second layer: 136˚, the laying angle of the third layer: 147˚, the laying angle of the fourth layer: 136˚, the laying angle of the fifth layer: 47˚, the laying angle of the

sixth layer: 156˚, the laying angle of the seventh layer: 72˚, and the laying angle of the eighth layer: 73˚.

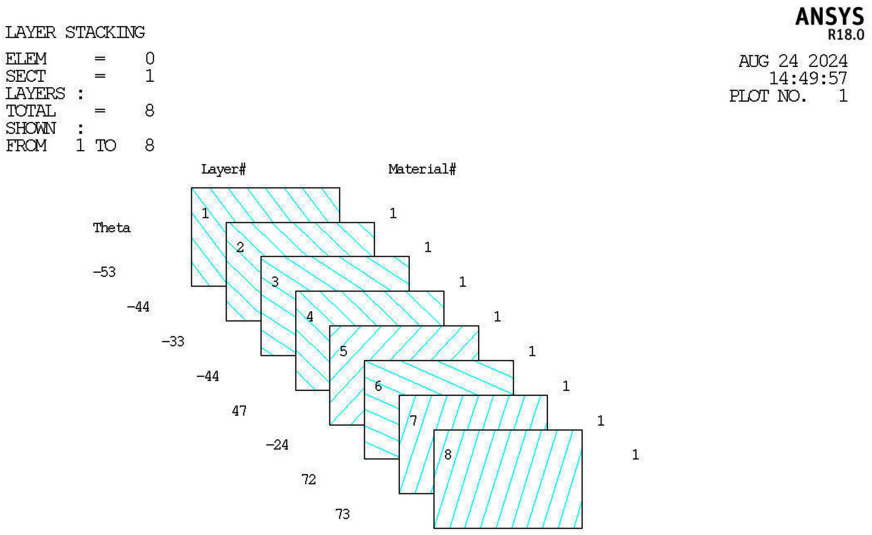

Figure 10. Schematic diagram of the ply angles.

As shown in **Figure 11**, it is the convergence diagram formed when the circular arc pressure vessel model uses the genetic algorithm for optimization calculation:

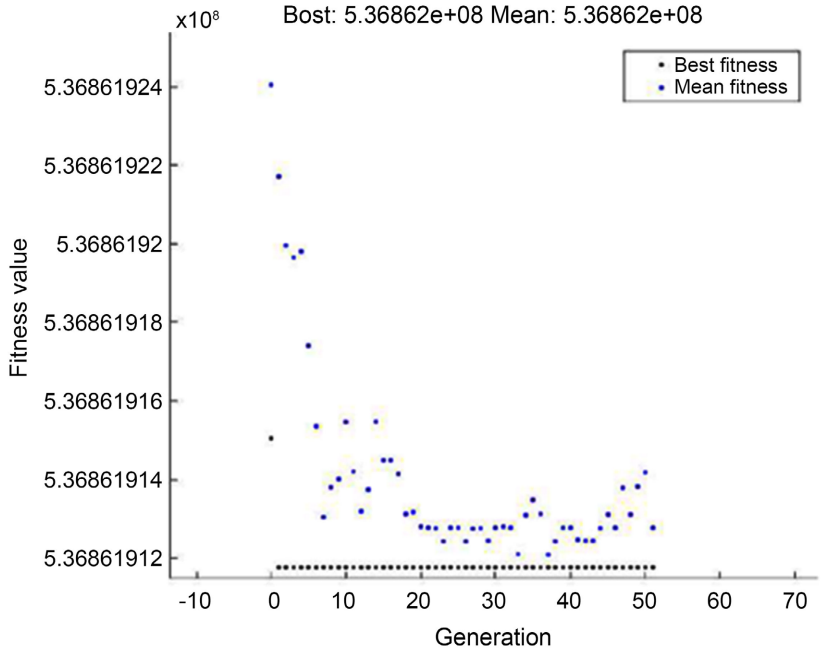

Figure 11. Convergence curve of the ply optimization of the circular arc pressure vessel.

According to **Figure 11**, it can be observed that although the best fitness value fluctuates to a certain extent near the average fitness value, the difference is relatively small and tends to converge at about the 51st generation, with a convergence

value of approximately 5.3685E+08 Pa.

As shown in Figure 12, it is the equivalent stress nephogram corresponding to the optimal laying angle. In this section, instead of considering the geometric shape, the optimization results of the geometric shape of the uniform material are used to optimize the laying angle of the composite ply. After the optimization calculation, the optimal laying angle was obtained. Then, the circular arc pressure vessel model as shown in Figure 12 was generated using the APDL parametric language, and the corresponding equivalent stress nephogram was generated. The figure shows that the deformation is 0.563E−03 m, the minimum equivalent stress value is 0.261E+09 Pa, and the maximum equivalent stress value is 0.537E+09 Pa. The gap between the two values indicates that the transition of the stress nephogram is relatively uniform.

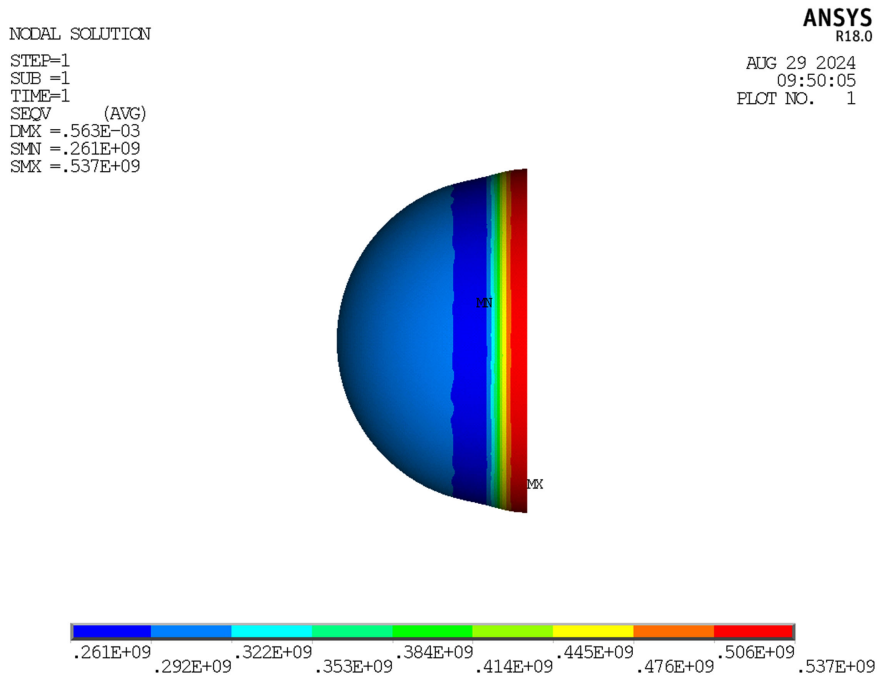

Figure 12. Equivalent stress nephogram under the optimal laying angle.

2) The results obtained by taking the optimal laying angle of the pressure vessel model as the target under the constraint of the laying angle of the elliptical pressure vessel model are shown in Table 3 below:

Table 3. Optimal laying angle and equivalent stress magnitude.

x_1	x_2	x_3	x_4	x_5	x_6	x_7	x_8	Equivalent stress (Pa)
71˚	160˚	77˚	149˚	63˚	54˚	25˚	168˚	5.1969e+08

After the optimization calculation through the genetic algorithm, the optimal angle data in the above table can be obtained. Figure 13 is the laying angle diagram of each layer:

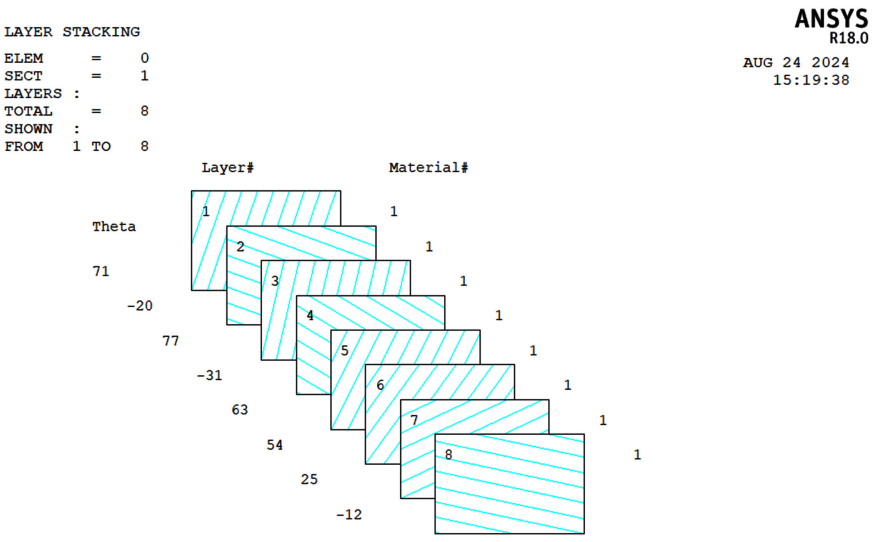

Figure 13. Schematic diagram of the optimal ply.

The SECPLOT command can be used to retrieve the arranged number of ply layers and laying angles. It can be observed from Figure 13 that the laying angle of the first layer is: 71˚, the laying angle of the second layer is: 160˚, the laying angle of the third layer is: 77˚, the laying angle of the fourth layer is: 149˚, the laying angle of the fifth layer is: 63˚, the laying angle of the sixth layer is: 54˚, the laying angle of the seventh layer is: 25˚, and the laying angle of the eighth layer is: 168˚.

As shown in Figure 14, it is the optimization convergence diagram formed when the elliptical pressure vessel model uses the genetic algorithm for optimization calculation:

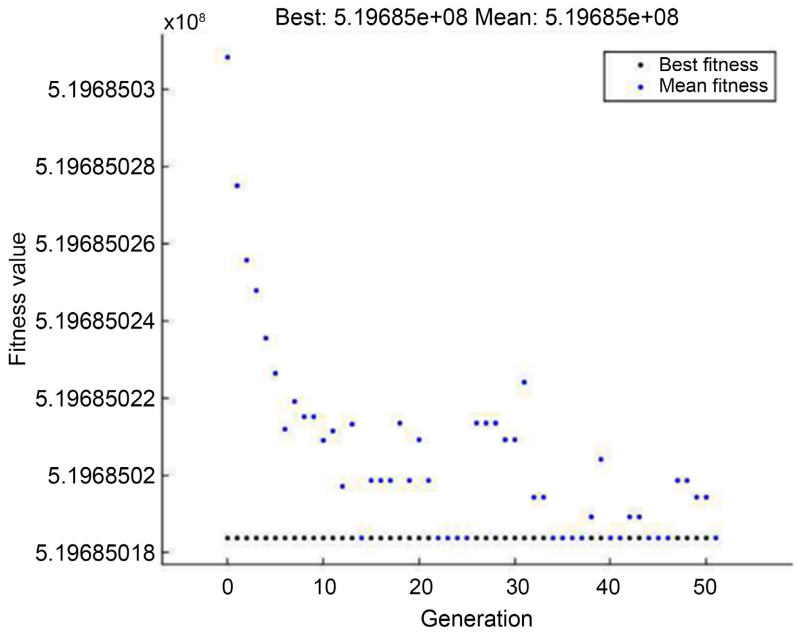

Figure 14. Convergence diagram.

When performing optimization calculations using the genetic algorithm, Figure 14 shows that the best fitness value fluctuates near the average fitness value. Although the difference is small, it eventually converges at 5.1969e+08 Pa.

As shown in Figure 15, it is the equivalent stress nephogram corresponding to the optimal laying angle:

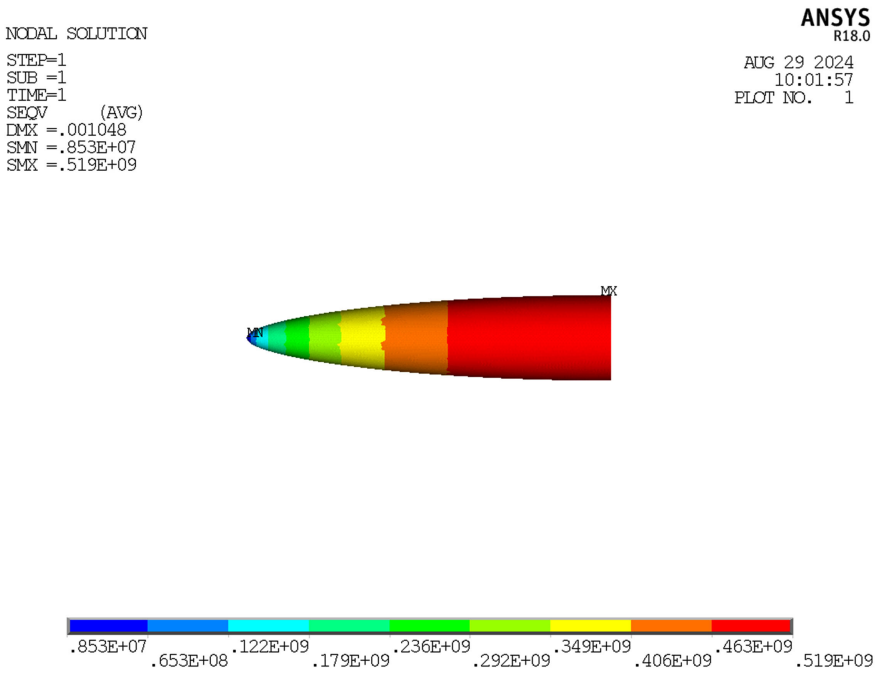

Figure 15. Equivalent stress nephogram under the optimal laying angle.

In this section, the geometric shape is not considered. Instead, the optimization results of the geometric shape of the uniform material are used to optimize the laying angle of the composite ply. It can be observed from the equivalent stress nephogram corresponding to the optimal laying angle shown in Figure 15 that the deformation of the elliptical pressure vessel is 0.002018 meters, the minimum equivalent stress value is 0.328E+07 Pa, and the maximum equivalent stress value is 0.520E+09 Pa. Due to the large gap between the maximum and minimum values, and it can be seen by observing the equivalent stress nephogram under the optimal laying angle that the stress distribution is not uniform. In this case, the elliptical pressure vessel is prone to damage, so the elliptical pressure vessel model is not applicable.

3) Under the constraints of the parabolic pressure vessel model, the obtained optimal laying angle and the corresponding magnitude of the equivalent stress value are shown in Table 4 below:

Table 4. Optimal angle and magnitude of equivalent stress value.

x_1	x_2	x_3	x_4	x_5	x_6	x_7	x_8	Equivalent stress (Pa)
6˚	79˚	40˚	111˚	84˚	97˚	24˚	88˚	5.8692e+08

Similarly, by using the SECPLOT command, the number of layers and laying angles of the parabolic pressure vessel model under the optimal laying angle can be retrieved. As shown in Figure 16, observed from left to right, the laying angle of the first layer is 6˚, the laying angle of the second layer is 79˚, the laying angle of the third layer is 40˚, the laying angle of the fourth layer is 111˚, the laying angle of the fifth layer is 84˚, the laying angle of the sixth layer is 97˚, the laying angle of the seventh layer is 24˚, and the laying angle of the eighth layer is 88˚.

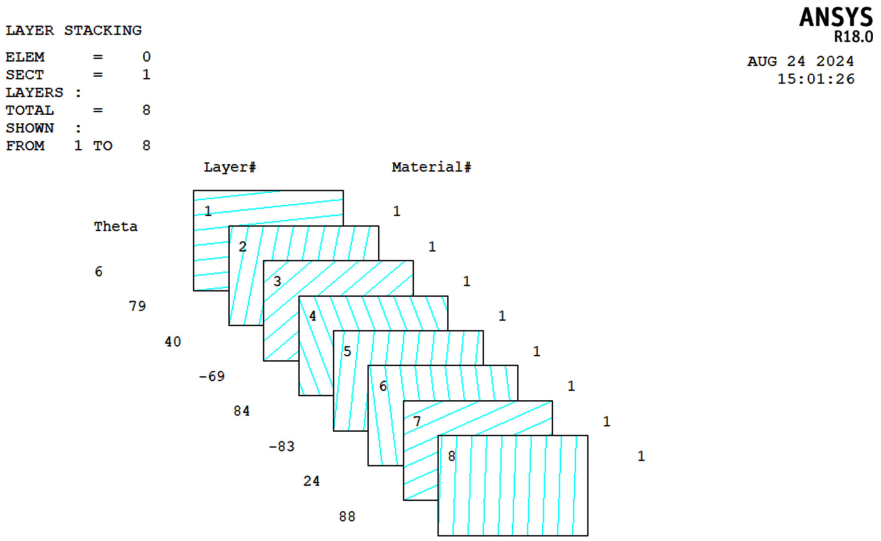

Figure 16. Schematic diagram of laying angle.

Figure 17 is the convergence curve diagram during the ply optimization design of the parabolic pressure vessel:

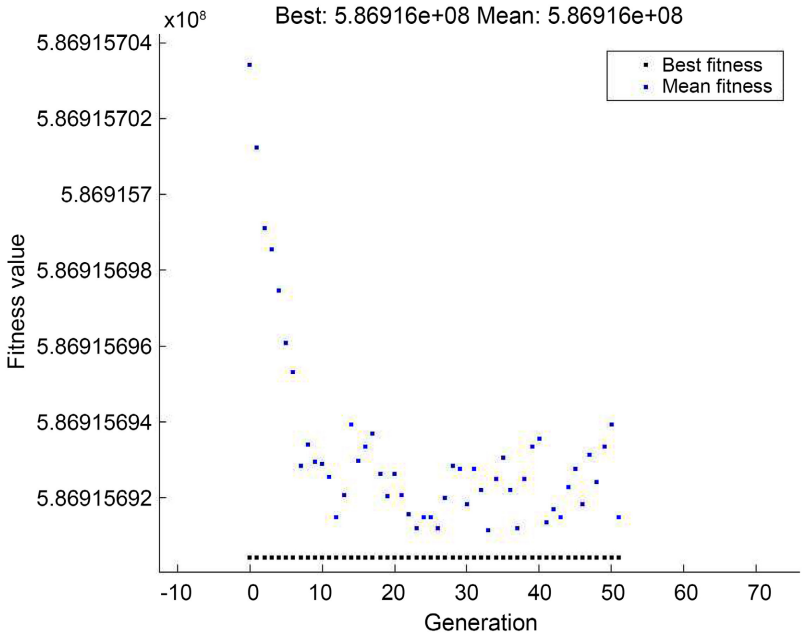

Figure 17. Optimization convergence curve.

It can be observed from Figure 17 that the best fitness value fluctuates around the average fitness value and finally converges at 5.8692e+08.

By observing Figure 18, it can be observed that the deformation of the parabolic pressure vessel is 0.773E−03 m, the maximum equivalent stress value is 0.109E+10 Pa, and the minimum equivalent stress value is 0.875E+08 Pa. Due to the large difference between the maximum and minimum values, it may cause more significant damage in the area with uneven stress distribution, which is inconsistent with the equivalent stress principle. Therefore, with the laying angle of the ply as the constraint condition, the parabolic model is not the optimal choice.

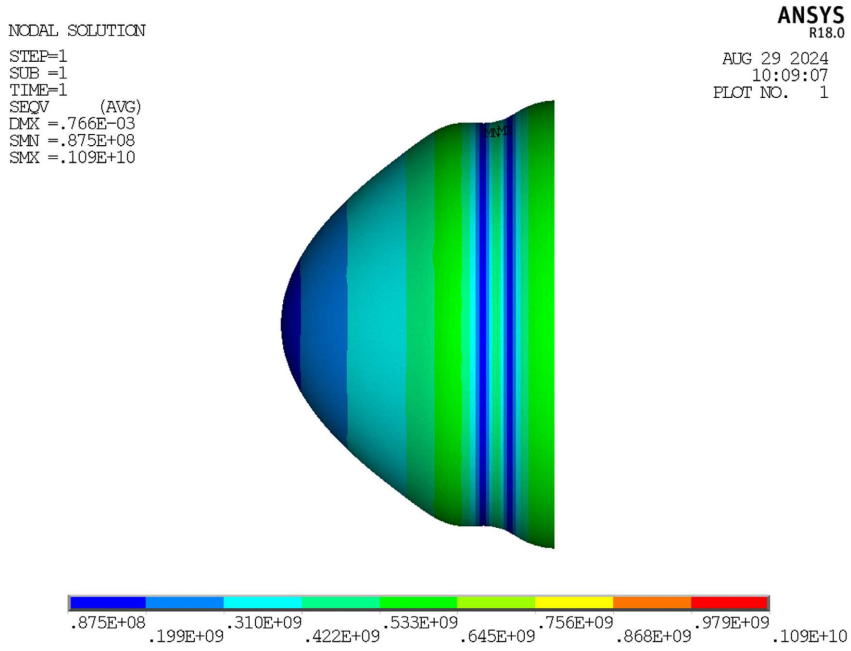

Figure 18. Equivalent stress nephogram corresponding to the optimal laying angle.

4) Under the constraint of the laying angle of the fitting curve model, the obtained optimal laying angle and the corresponding magnitude of the equivalent stress value are shown in Table 5 below:

Table 5. Optimal angle and magnitude of equivalent stress value.

x_1	x_2	x_3	x_4	x_5	x_6	x_7	x_8	Equivalent stress (Pa)
175˚	127˚	136˚	27˚	136˚	47˚	156˚	72˚	5.36862e+08

Figure 19 is the optimization convergence graph obtained when performing the optimization calculation using the genetic algorithm.

By using the SECPLOT command, the number of ply layers and the corresponding laying angles of the fitting curve-shaped pressure vessel model under the optimal laying angle can be retrieved. As shown in Figure 20, it is the retrieved relevant information about the ply layers and laying angles. Through observing the information in the figure, it can be obtained that the laying angle of the first layer is: 175˚, the laying angle of the second layer is: 127˚, the laying angle of the

third layer is: 136˚, the laying angle of the fourth layer is: 27˚, the laying angle of the fifth layer is: 136˚, the laying angle of the sixth layer is: 47˚, the laying angle of the seventh layer is: 156˚, and the laying angle of the eighth layer is: 72˚.

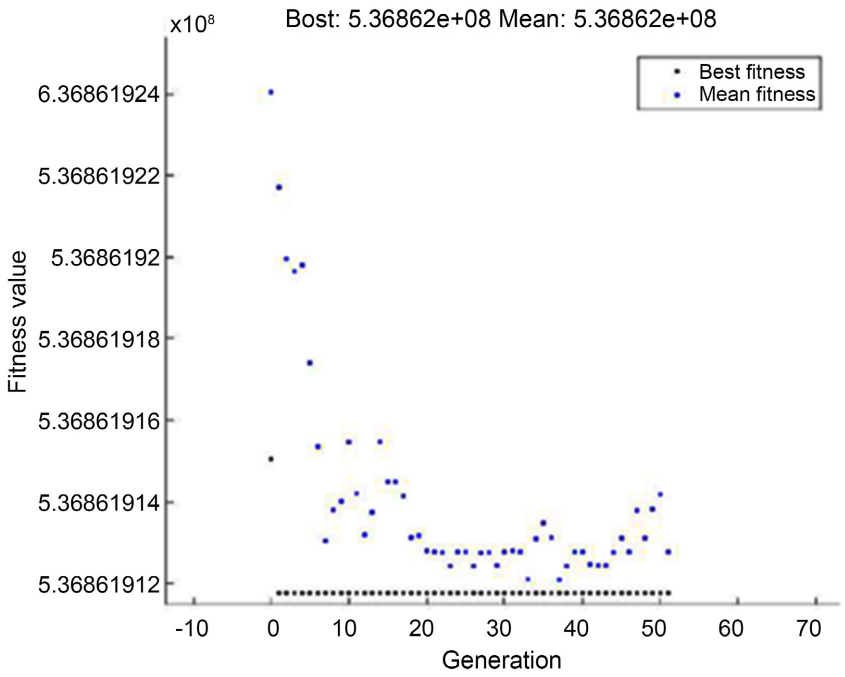

Figure 19. Optimization convergence diagram.

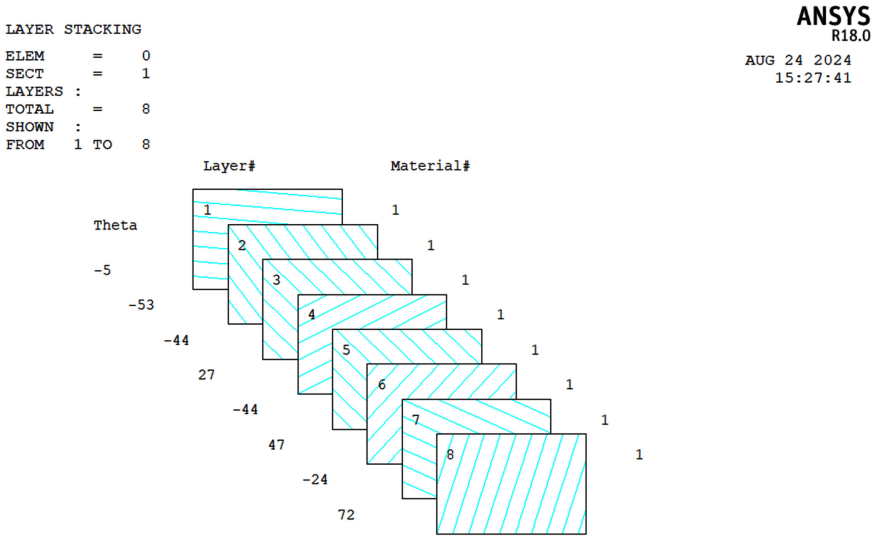

Figure 20. Schematic diagram of the optimal laying angle

By observing the equivalent stress nephogram corresponding to the optimal laying angle in Figure 21, the deformation of the fitting curve-shaped pressure vessel is 0.568E−03 m, the minimum equivalent stress value is 0.261E+09 Pa, and the maximum equivalent stress value is 0.537E+09 Pa. The ratio of the two is 0.48, which is more in line with the equivalent stress criterion. The stress distribution

is relatively uniform, and there is no significant stress concentration phenomenon in the equivalent stress nephogram.

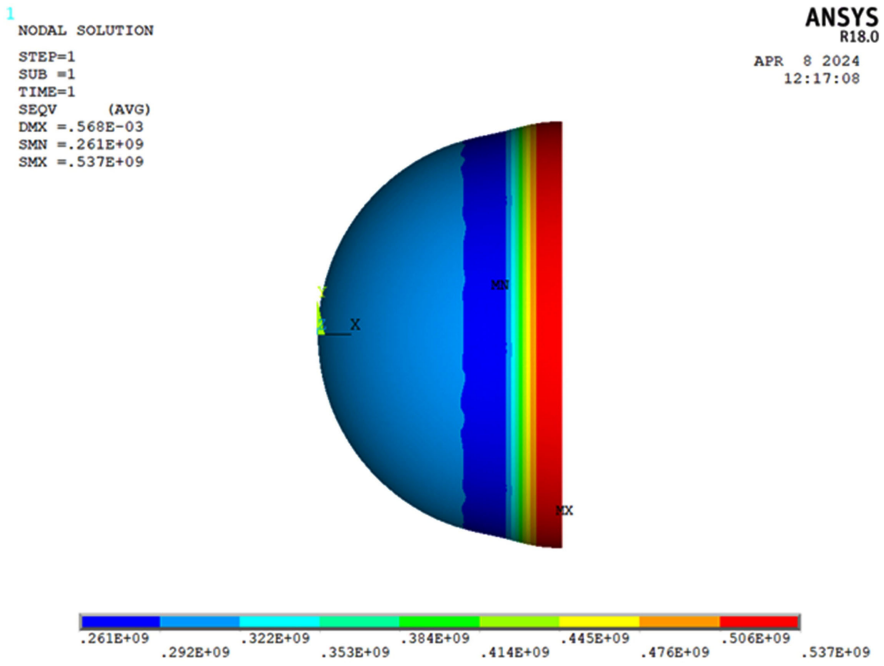

Figure 21. Equivalent stress nephogram corresponding to the optimal laying angle.

By comparing the equivalent stress nephograms of various pressure vessel models, it is found that the fitting curve-shaped pressure vessel model is relatively more suitable. The fitting curve of this model can adapt to a variety of models, including parabolas, arcs, ellipses, and other models. Considering the wide applicability of the fitting curve, in composite materials, especially when considering the ply angle, the fitting curve-shaped pressure vessel model is more practical.

5. Conclusion

In this study, with the help of APDL parametric modeling and genetic algorithm, the ply angles of composite pressure vessels of different shapes were optimized and calculated. The research results show that the equivalent stress corresponding to the optimal laying angle of the arc-shaped pressure vessel is 5.3685e+08 Pa, the elliptical one is 5.1969e+08 Pa, the parabolic one is 5.8692e+08 Pa, and the fitting curve-shaped one is 5.36862e+08 Pa. The stress distribution of the fitting curve-shaped pressure vessel is relatively uniform, with a deformation of 0.568E−03 m, a minimum equivalent stress value of 0.261E+09 Pa, a maximum equivalent stress value of 0.537E+09 Pa, and a ratio of 0.48, which conforms to the equivalent stress criterion. In addition, its fitting curve can adapt to a variety of models and has higher practical value. However, the stress distribution of elliptical and parabolic pressure vessels is uneven, and their applicability is poor. In the future, the application of the fitting curve model in composite materials can be further explored to optimize the design of pressure vessels.

Conflicts of Interest

The authors declare no conflicts of interest regarding the publication of this paper.

References

[1] Regassa, Y., Gari, J. and Lemu, H.G. (2022) Composite Overwrapped Pressure Vessel Design Optimization Using Numerical Method. *Journal of Composites Science*, **6**, Article No. 229. https://doi.org/10.3390/jcs6080229

[2] Park, Y.H. and Sakai, J. (2019) Optimum Design of Composite Pressure Vessel Structure Based on 3-Dimensional Failure Criteria. *International Journal of Material Forming*, **13**, 957-965. https://doi.org/10.1007/s12289-019-01519-x

[3] Park, Y.H. and Sakai, J. (2019) Optimum Design of Composite Pressure Vessel Structure Based on 3-Dimensional Failure Criteria. *International Journal of Material Forming*, **13**, 957-965. https://doi.org/10.1007/s12289-019-01519-x

[4] Hajmohammad, M.H., Tabatabaeian, A., Ghasemi, A.R. and Taheri-Behrooz, F. (2020) A Novel Detailed Analytical Approach for Determining the Optimal Design of FRP Pressure Vessels Subjected to Hydrostatic Loading: Analytical Model with Experimental Validation. *Composites Part B*: *Engineering*, **183**, Article ID: 107732. https://doi.org/10.1016/j.compositesb.2019.107732

[5] Fathallah, E. and Helal, M. (2019) Finite Element Modelling and Multi-Objective Optimization of Composite Submarine Pressure Hull Subjected to Hydrostatic Pressure. *IOP Conference Series*: *Materials Science and Engineering*, **683**, Article ID: 012072. https://doi.org/10.1088/1757-899x/683/1/012072

[6] Sakai, J. and Park, Y.H. (2019) Optimum Design of Composite Pressure Vessel Based on 3-Dimensional Failure Criteria. *ASME* 2019 *Pressure Vessels & Piping Conference*, San Antonio, 14-19 July 2019, V002T02A030. https://doi.org/10.1115/pvp2019-93816

[7] Wu, C., Gao, Y., Fang, J., Lund, E. and Li, Q. (2019) Simultaneous Discrete Topology Optimization of Ply Orientation and Thickness for Carbon Fiber Reinforced Plastic-Laminated Structures. *Journal of Mechanical Design*, **141**, Article ID: 044501. https://doi.org/10.1115/1.4042222

[8] Vafaeesefat, A. and Khani, A. (2007) Head Shape and Winding Angle Optimization of Composite Pressure Vessels Based on a Multi-Level Strategy. *Applied Composite Materials*, **14**, 379-391. https://doi.org/10.1007/s10443-008-9052-8

[9] Iwasaki, K.M.K., Reis, P.A., Oliveira, L.G., Rauber, W.K. and De Medeiros, R. (2023) Methodology to Analyse Carbon Fibre/Epoxy Composite Pressure Vessel Based on Finite Element Modelling and Classical Laminated Theory. *Journal of the Brazilian Society of Mechanical Sciences and Engineering*, **45**, Article No. 336. https://doi.org/10.1007/s40430-023-04260-4

[10] Matos, H., Chaudhary, B. and Ngwa, A.N. (2022) Optimization of Composite Cylindrical Shell Structures for Hydrostatic Pressure Loading. *Journal of Pressure Vessel Technology*, **145**, Article ID: 011504. https://doi.org/10.1115/1.4055159

[11] Mia, R., Shuva, I.B., Mamun, A.A., Bakar, A., Rumman, F.I. and Rahman, M. (2020) The Fabrication of Composite Material Based on Natural Macromolecules: A Review. *Open Access Library Journal*, **7**, e6977. https://doi.org/10.4236/oalib.1106977

[12] Adeyefa, O. and Oluwole, O. (2013) Finite Element Modeling of Variable Membrane Thickness for Field Fabricated Spherical (LNG) Pressure Vessels. *Engineering*, **5**, 469-474. https://doi.org/10.4236/eng.2013.55056